Nucl. Fusion **51** (2011) 094025 (9pp) doi:10.1088/0029-5515/51/9/094025

Studying ignition schemes on European laser facilities

S. Jacquemot[1,2], F. Amiranoff[1], S.D. Baton[1], J.C. Chanteloup[1], C. Labaune[1], M. Koenig[1], D.T. Michel[1], F. Perez[1], H.P. Schlenvoigt[1], B. Canaud[2], C. Cherfils Clérouin[2], G. Debras[2], S. Depierreux[2], J. Ebrardt[2], D. Juraszek[2], S. Lafitte[2], P. Loiseau[2], J.L. Miquel[2], F. Philippe[2], C. Rousseaux[2], N. Blanchot[3], C.B. Edwards[4], P. Norreys[4], S. Atzeni[5], A. Schiavi[5], J. Breil[6], J.L. Feugeas[6], L. Hallo[6], M. Lafon[6], X. Ribeyre[6], J.J. Santos[6], G. Schurtz[6], V. Tikhonchuk[6], A. Debayle[7], J.J. Honrubia[7], M. Temporal[7], D. Batani[8], J.R. Davies[9], F. Fiuza[9], R.A. Fonseca[9], L.O. Silva[9], L.A. Gizzi[10], P. Koester[10], L. Labate[10], J. Badziak[11] and O. Klimo[12]

[1] LULI, Ecole Polytechnique, CNRS, CEA, UPMC, 91128 Palaiseau cedex, France
[2] CEA, DAM, DIF, F-91297 Arpajon, France
[3] CEA, DAM, CESTA, F-33114 Le Barp, France
[4] Central Laser Facility, STFC Rutherford Appleton Laboratory, Didcot, Oxfordshire, OX11 0QX, UK
[5] Dipartimento SBAI, Università di Roma 'La Sapienza' and CNISM, via A. Scarpa 14, 00161 Roma, Italy
[6] CELIA, Université Bordeaux I, CNRS, CEA, 351 cours de la libération, 33405 Talence, France
[7] ETSI Aeronáuticos, Universidad Politécnica de Madrid, 28040 Madrid, Spain
[8] Dipartimento di Fisica 'G.Occhialini', Università di Milano-Bicocca and CNISM, 20126 Milano, Italy
[9] GoLP/Instituto de Plasmas e Fusao Nuclear, Instituto Superior Técnico, 1049001 Lisbon, Portugal
[10] ILIL, Istituto Nazionale di Ottica, UOS 'Adriano Gozzini', CNR, via G. Moruzzi 1, 56124 Pisa, Italy
[11] Institute of Plasma Physics and Laser Microfusion, EURATOM Association, 00-908, Warsaw, Poland
[12] Czech Technical University, Faculty of Nuclear Sciences and Physical Engineering, 11519 Prague, Czech Republic

E-mail: sylvie.jacquemot@polytechnique.fr

Received 27 January 2011, accepted for publication 9 March 2011
Published 31 August 2011
Online at stacks.iop.org/NF/51/094025

Abstract
Demonstrating ignition and net energy gain in the near future on MJ-class laser facilities will be a major step towards determining the feasibility of *Inertial Fusion Energy* (IFE), in Europe as in the United States. The current status of the French *Laser MégaJoule* (LMJ) programme, from the laser facility construction to the indirectly driven central ignition target design, is presented, as well as validating experimental campaigns, conducted, as part of this programme, on various laser facilities. However, the viability of the IFE approach strongly depends on our ability to address the salient questions related to efficiency of the target design and laser driver performances. In the overall framework of the European HiPER project, two alternative schemes both relying on decoupling target compression and fuel heating—fast ignition (FI) and shock ignition (SI)—are currently considered. After a brief presentation of the HiPER project's objectives, FI and SI target designs are discussed. Theoretical analysis and 2D simulations will help to understand the unresolved key issues of the two schemes. Finally, the on-going European experimental effort to demonstrate their viability on currently operated laser facilities is described.

1. Introduction

The first experiments on the National Ignition Facility (NIF) [1] in the United States successfully began in 2009. This major milestone gives confidence in demonstrating ignition and net energy gain within the next two years. Such an achievement will be a major step towards determining the feasibility of inertial confinement fusion (ICF) as an

Figure 1. Views of (left) one of the two completed LMJ laser halls and (right) the target chamber with some of its surrounding mechanical support components.

option for a carbon-free and sustainable energy source. The European horizon is then dual: first trustfully demonstrate indirectly driven laser ignition at the MJ energy level on LMJ [2] in France, thanks to an improved target design and a series of validating experiments, and then coordinate all the efforts towards IFE, in the framework of the ambitious HiPER project or the EURATOM IFE keep-in-touch activities, which currently support numerical and experimental studies of alternative ignition schemes and innovative technologies.

2. Current status of the CEA ICF programme

2.1. The LMJ laser facility

The LMJ project was launched in the 1990s and is now close to completion. Located in the Aquitaine region, at CEA/CESTA, the facility was designed to deliver on target up to 1.8 MJ and 550 TW of UV light (0.35 μm), in up to 240 laser beams (arranged in 30 bundles), with pulse shaping capabilities and duration from a few hundred picoseconds to 25 ns. The 1.68 hm^3 building was commissioned at the end of 2008; half of the four laser bays are now fully equipped (figure 1, left), the assembly of the remaining part being in progress. The target chamber (a 140 ton, 10 m diameter vacuum vessel) was installed in the target bay in November 2006, and the surrounding mechanical frameworks are currently progressively implemented (figure 1, right). In parallel, the feasibility of the fusion target fabrication was demonstrated. The main equipment (thermal shield positioner and extractor, cryogenic target positioner and cryogenic transfer unit) was validated and a cryogenic target assembly prototype is undergoing full characterization: experiments on layering of solid deuterium in an integrating sphere have for instance demonstrated that ice roughness can meet specifications [2, 3].

2.2. The ignition target design

The main approach for achieving ignition on LMJ relies on the indirect drive (ID) central ignition scheme. The first baseline target design (from which LMJ was designed) leads to a net gain $G \sim 16$; it consists of a DT capsule, with a uniformly germanium-doped plastic ablator, located inside a cylindrical gold cavity filled with a low-density gas, operating at 300 eV [4].

But, in order to explore the large LMJ parameter space, a variety of ignition targets, linked to different strategies of risk mitigation, have been recently designed. High-yield (20 MJ) fusion targets requiring no more than 1.2 MJ of laser energy (330 TW) have for instance been identified, allowing the first attempts to achieve ignition in a 160-beam two-cone configuration. They take advantage of graded-doped capsules and advanced rugby-shaped cocktail hohlraums. More precisely, the uranium-gold composite, from which the cavity is made, allows improving the hohlraum energetics by filling in the 'holes' of the absorption spectra, and thus increasing the mean Rosseland opacity [5], while the prolate-spheroid shape improves the coupling efficiency by minimizing the cavity wall surface (and thus the wall losses) [6, 7] and furthermore better controlling the radiation drive asymmetry on the capsule [8]. As for the use, for the capsule, of a gradually doped plastic ablator, it leads to a better robustness by controlling radiation preheating and enhancing tolerance to initial ablator roughness, consequently reducing sensitivity to Rayleigh–Taylor instabilities (RTIs) [9].

2.3. The preparatory experimental programme

As part of this programme to validate the above-described design and to better ensure success in achieving ignition, a series of experimental campaigns was conducted, either in France, at CEA on the LMJ quadruplet (four beams) prototype, the Ligne d'Intégration Laser (LIL) and at Ecole Polytechnique on LULI2000, or in the United States, at LLE on OMEGA.

Special attention has first been paid to experiments aiming at characterizing high-energy laser interaction with plasmas to quantify risks linked to parametric instabilities, such as stimulated Raman scattering (SRS) and stimulated Brillouin scattering (SBS), and to validate the optical longitudinal smoothing technique that will be implemented on LMJ. Two specific targets were designed for the occasion: a long open 'tube', to mimic the propagation of the inner laser cone into the homogeneous low-density gas medium (where SRS can develop), and a half-hohlraum, representative of the external cone propagation at the cavity wall–gas interface (where SBS can occur). Measurements performed on the LIL with the help of an elliptical Spectralon diffuser at LMJ-relevant intensities ($\sim 5 \times 10^{14}$ W cm^{-2}) and pulse durations, with a 14 GHz phase modulation added to the intrinsic optical longitudinal smoothing, exhibit moderate (less than 13%, i.e. within the design margins) SRS and SBS absolute reflectivities (figure 2).

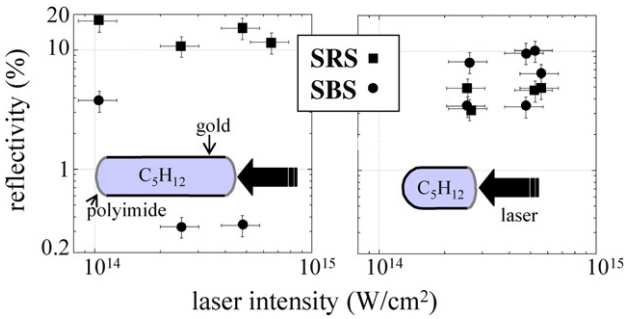

Figure 2. Absolute SRS (squares) and SBS (bullets) time-integrated reflectivities as a function of the LIL laser intensity and schematic drawing of the half-hohlraum (right) and tube (left) targets: moderate values are recorded at LMJ-relevant intensities ($\sim 5 \times 10^{14}$ W cm^{-2}).

(This figure is in colour only in the electronic version)

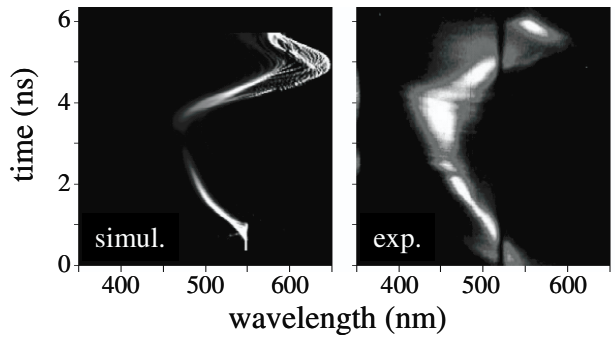

Figure 3. Time-resolved Raman spectra calculated (left) and recorded (right) on the LIL for a laser intensity of 5×10^{14} W cm^{-2}, showing similar features.

The observed temporal and spectral features, signature of a complex hydrodynamics, were successfully reproduced by simulations coupling 2D radiative-hydro-computations and linear gain calculations (figure 3).

Ignition demonstration will be based on 3ω (0.35 μm) laser–matter interaction but it was shown that 2ω (0.53 μm) operation may hold significant advantages: increased target design domain, lower maintenance costs due to higher optics damage threshold, etc if the level of scattering instabilities is kept low. A series of experiments on the LULI2000 laser facility was designed to check this assumption; its results indicate that the laser wavelength does not affect the final SBS level at saturation and for moderate ion acoustic wave damping [10].

In the ID ignition scheme, as in the direct drive one, the central hot spot formation follows an isentropic compression of the capsule due to spherical convergence of accurately timed shock waves (four or five shocks, depending on the target design). Two velocity interferometry systems for any reflector (VISARs) at 1.064 (ω) and 0.532 μm (2ω), for shock velocity measurements with a 1% precision, and a rear-surface self-emission 1D time-resolved imaging system were commissioned in order to conduct on the LIL facility preliminary shock timing experiments on planar targets. The dynamics of the first two shocks has then been reproduced using a LMJ-relevant radiation drive.

Finally, the concept of rugby-shaped hohlraums to enhance the x-ray drive in indirectly driven capsule implosions

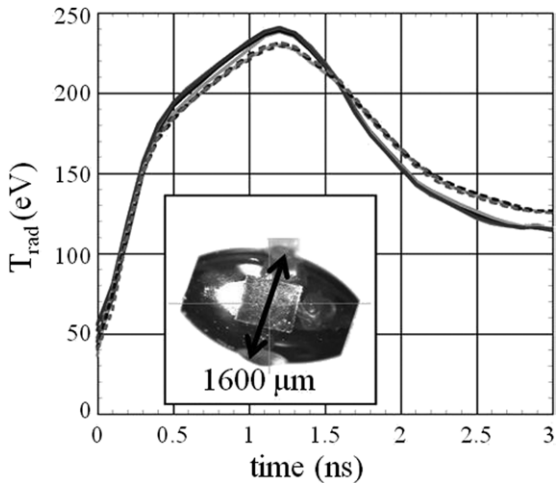

Figure 4. Measured radiation temperature histories for rugby-shaped (solid lines) and cylindrical (dotted lines) gold hohlraums, driven with 40 laser beams delivering ~20 kJ in 1 ns, and picture of one of the rugby-shaped targets for which a slight increase in the maximum temperature is exhibited.

has recently been tested in a series of shots on the OMEGA laser facility, in collaboration with LLNL and MIT. When compared with cylindrical hohlraums with equivalent radius and laser entrance aperture (figure 4), the rugby-shaped hohlraums exhibit a significant (+16%) increase in the x-ray flux despite higher SBS backscattering energy losses. Such a high-performance design has led, on 20 kJ-driven D_2 implosions, to a record neutron yield of 1.5×10^{10} [11] and to the first D_2 burn history measurements and the first neutron images in ID.

3. The HiPER project

The HiPER project, accepted on the European roadmap in October 2006, is a proposed European High Power Laser Energy Research facility dedicated to demonstrating the feasibility of laser-driven fusion as a future energy source [12] (figure 5, left).

During the present preparatory phase (2008-2011), 26 European partners share expertise to address the main scientific issues. The corresponding physics roadmap is describing the experimental, numerical and theoretical studies to be pursued to down-select the most efficient 'alternative' (to contrast with 'nominal' ID) ignition scheme. This important mission is supported by an access program to large-scale laser facilities available inside and outside Europe, including PETAL, the multi-kJ PW laser facility planned to be coupled with LMJ in a few years [13] (figure 5, right).

Once fuel ignition demonstrated, on NIF and then on LMJ, the HiPER strategy will be to address technological challenges to advance on the route to a real high-power fusion reactor device. Mainly linked to operation at high repetition rate, the studies that will be undertaken during this next phase will aim at developing key engineering prototypes, such as a 10 kJ/a few Hz beamline or systems devoted to high-precision target injection, tracking and engagement. The reactor concept itself will also be the subject of a detailed analysis dealing with the

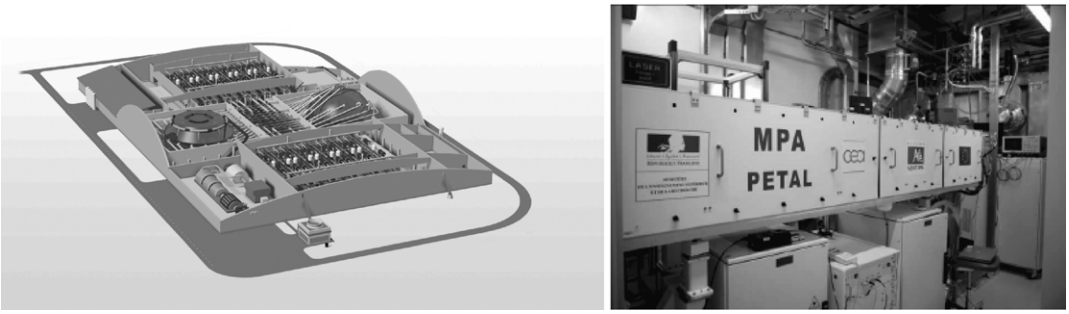

Figure 5. Artistic view of the HiPER facility (left) and PETAL pre-amplification module (right).

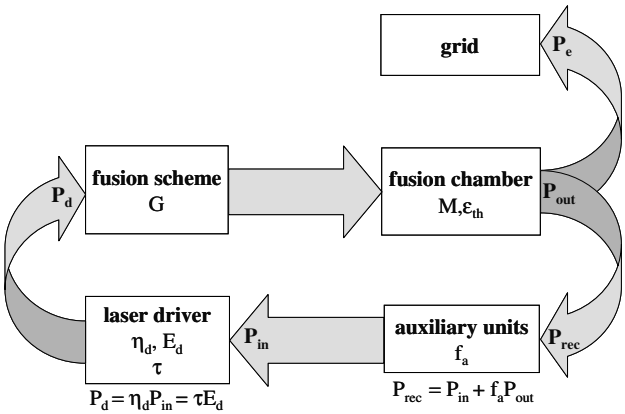

Figure 6. Generic IFE power flow diagram: assuming reasonable values for the involved parameters (driver efficiency $\eta_d = 0.15$, overall energy multiplication factor $M = 1.1$, thermal conversion efficiency $\varepsilon_{th} = 0.4$ and auxiliary power fraction $f_a = 0.1$), an 'alternative' laser driver of energy 0.6 MJ (E_d) and repetition rate 21 Hz allows delivering an electrical power to the grid of 0.4 GWe (P_e) if a target gain (G) of the order of 100 can be achieved; note that the recirculating power fraction (P_{rec}/P_{out}) is then 26%, close to the 20% value often cited goal for IFE from the economical point of view).

choice of the chamber materials (able to support large particle and radiation fluxes), remote handling, etc.

The HiPER business case, including the final reactor design and a cost analysis, should be ready by the end of the decade before entering the construction phase. The power-to-grid demonstration is expected at the horizon of 2035–2040 after testing key reactor components.

4. The 'alternative' ignition schemes

In the overall framework of the European HiPER project, two 'alternative' schemes—fast ignition (FI) and shock ignition (SI)—are currently considered. They both rely on decoupling *direct drive* target compression from fuel heating (and thus ignition), using, as an external match, either a PW-class laser-accelerated fast particle beam or a strong convergent shock. They both can potentially lead to very high gains, ∼100, as required by a IFE 0.4 GW reactor (figure 6).

The shared baseline target is an all-DT capsule, of external radius 1044 μm and a shell thickness of 211 μm, irradiated by a sequence of laser pulses: a short intense (∼3 kJ) picket, for low adiabat shaping, a shaped multi-nanosecond ∼180 kJ pulse, to implode the target at moderate velocity, and a precisely timed, shorter and intense ignition pulse. For the time being, a 48-beam (3 rings) irradiation scheme is proposed for the direct drive compression phase [14].

As irradiation non-uniformities have to be carefully controlled to minimize low-mode capsule perturbation they could seed, a specific 3D illumination code, named CECLAD, was developed to determine the laser mode spectrum thanks to a Legendre polynomial expansion. Post-processing by 2D multimode simulations allows assessing the hydrodynamic target stability and the scheme robustness. It was shown that ignition can be achieved despite a maximum capsule deformation at the internal DT solid–gas interface of ∼10 μm peak-to-valley, with an average non-uniformity (σ_{rms}) close to 1% under moderate power imbalance (σ_{PI}) and laser pointing error (σ_{PE}) [14–16]. Once the dimensions of the super-Gaussian laser focal spots carefully optimized, the (σ_{PI}, σ_{PE}) parameter space can be noticeably enlarged and σ_{rms} lowered [17].

It has been furthermore proposed to reduce laser imprint with the help of a low-density foam coating of the fuel capsule. Experiments conducted on the LIL facility have confirmed that an ionization wave, propagating faster than the laser-driven shock, can decrease pressure fluctuations at the ablation surface, thus leading to efficient plasma-induced beam smoothing [18].

4.1. Fast ignition studies

The current nominal design assumes production of a fast and energetic electron beam by interaction of a high-energy multi-PW (∼70 kJ/10–20 ps) laser pulse with the tip of a re-entrant double gold cone. This cone is mainly used to keep a path free of plasma and allow efficient particle generation close to the compressed core. Although it breaks spherical symmetry, this can be tolerated because ignition will occur through direct particle energy deposition into the fuel.

A set of inter-connected 2D numerical (radiation hydrodynamic, PIC and transport) codes was developed to properly describe such a scheme. It has notably been used to study the cone tip survival and has exhibited the importance of an asymmetric irradiation [19] as well as the influence of the radial profile of the fast electron beam on its magnetic collimation [20, 21] (figure 7).

Unacceptable high divergence (up to 55°) of the laser-accelerated electron beam was calculated for realistic

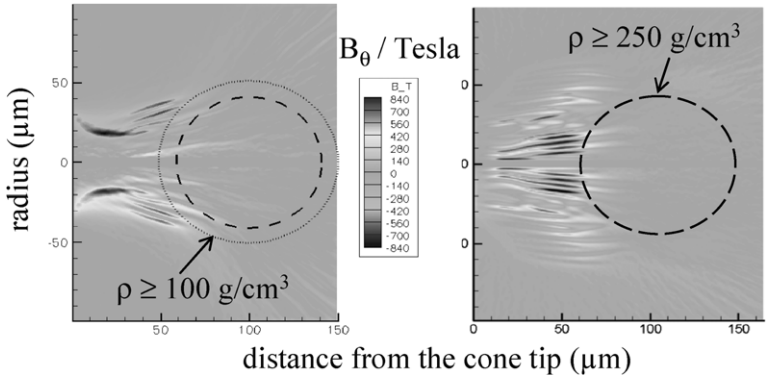

Figure 7. 2D maps of the azimuthal magnetic field (B_θ) generated at the end of the laser pulse without (left) or with (right) taking into account the electron transverse velocity: they clearly show that the magnetic collimation could be strongly overestimated when non-realistic conditions are taken into account.

transverse profiles, moreover leading to an increase in the estimated ignition energy threshold by a factor $1/[1-\theta_r/\Delta\theta_0]$ if the local electron angular distribution is approximated by a Gaussian function $\propto \exp[-(\theta-\theta_r)^2/\Delta\theta_0^2]$. Some improvements could still be done (reducing the divergence down to, at least, 35°) by means of optimized designs of the cone and of the spatial-temporal laser profiles.

In parallel, the first self-consistent modelling of FI was performed at realistic scales, i.e. for times up to 20 ps, length scales on the order of the compressed target radius, and realistic density/temperature profiles, thanks to the development of a hybrid version of the OSIRIS PIC code [22].

On the experimental point of view, two collaborative campaigns were conducted on LULI2000 and on VULCAN at the Rutherford Appleton Laboratory (RAL) to study fast electron transport.

The first experiment aimed at systematically studying the dependence of the laser energy absorption (at peak irradiance on target close to 4×10^{19} W cm^{-2}) and fast electron acceleration on laser intensity and plasma density scale lengths, produced by either varying the duration of the laser pedestal at ω (which led to energy contrast ranging from 3×10^{-3}, at the best, to 10^{-2}, at the worst) or frequency doubling (2ω) [23]. A rather complete set of plasma diagnostics was implemented; it included in particular a well-characterized Cu Kα imager, to trace the laser-accelerated electron beam passing through a fluorescence layer embedded in the target, and transverse interferometry, to visualize plasma expansion and provide an estimate of the plasma scale length. A reduction in the electron beam spread, which could be associated with a decrease in the divergence, was clearly observed when the plasma gradients steepened (figure 8).

The RAL experiment was the first European campaign devoted to fast electron transport in cylindrically compressed matter (in contrast with previous planar experiments described in [24]).

Four long-pulse (50 J/1 ns) laser beams were used to radially compress a plastic cylinder filled with a low-density foam and closed with two metallic foils (Ni at the front, Cu at the rear). A fast electron beam was generated by a fifth short-pulse (160 J/10 ps) laser beam irradiating the entrance foil (figure 9) [25, 26].

Transverse x-ray and proton radiography were implemented to measure the time evolution of the tube diameter;

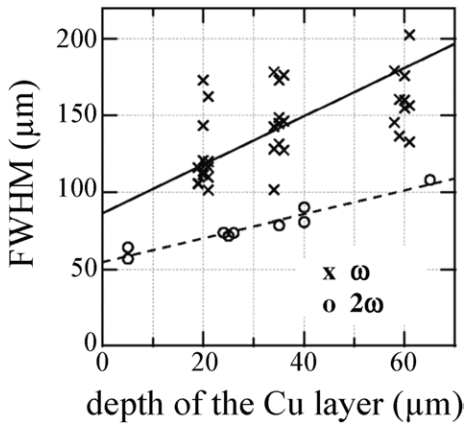

Figure 8. Fast electron beam size—from Cu Kα imaging—as a function of the emitter depth (or the electron propagation length) for various plasma density scale lengths (or laser contrast ratios) showing a reduction in the electron beam spread when gradients relax (at 2ω).

they provided valuable information to benchmark radiation hydrodynamic codes (figure 10) and thus allowed inferring the density and the temperature of the compressed foam into which the fast electrons propagate.

2D Cu Kα side-on imaging gave an insight of the electron beam spread which appears to be very sensitive to the electron injection timing. 2D hybrid simulations allowed explaining such behaviour; they revealed complex interaction between the electrons and the self-generated magnetic fields. Before stagnation, due to the presence of strong resistivity gradients, these latter collimate the fast electron beam, while, at stagnation, the laser-induced shock converging to the cylinder centre, the gradients are smoothed and the electron beam starts diverging (figure 11).

4.2. Shock ignition studies

In the case of SI, a properly timed strong shock is launched by a laser spike with a duration of a few hundred picoseconds. Once amplified thanks to spherical convergence and collision with an outward directed rebound shock, it can lead to high central pressures and hot spot formation. Such a situation corresponds to a non-isobaric fuel assembly which requires less energy to ignite that does the isobaric conventional central ignition one.

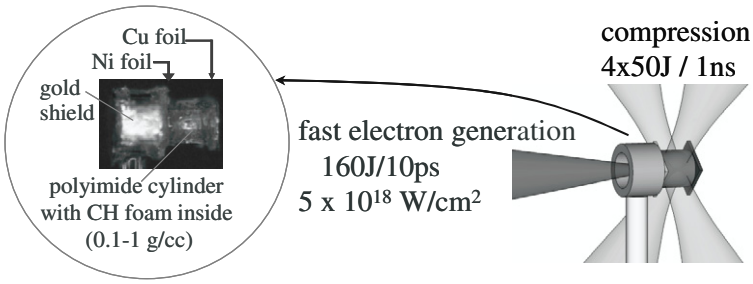

Figure 9. Sketch of the VULCAN experimental set-up.

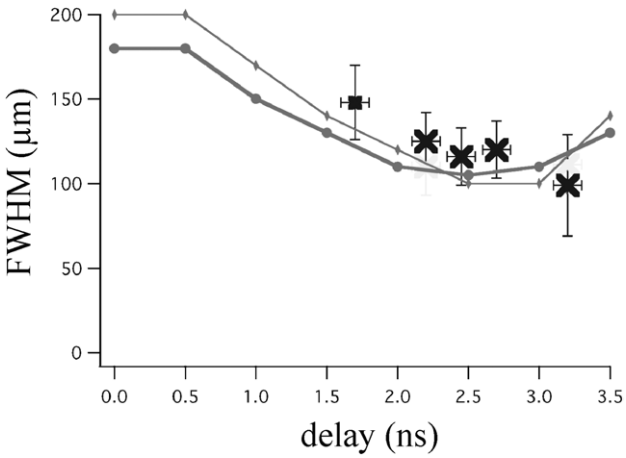

Figure 10. Time evolution of the tube diameter as calculated by the CHIC code (curves) and measured during the RAL experiment (crosses and square): a reasonably good agreement is exhibited at times close to maximum compression (2.2 ns).

This feature makes the SI scheme especially appealing for IFE. Radiation hydrodynamic simulations have shown that, for the baseline HiPER target, a gain close to 90 can be achieved, with only 280 kJ of incident laser energy at 3ω (including 100 kJ in a 500 ps-long spike). Furthermore, a rather wide (∼250 ps) ignition window (time interval into which the spike has to be launched to ensure at least 80% of the maximum yield) was estimated [27].

Theoretical modelling of the SI gain curves and of the relationship between the intensity of the required laser spike and the implosion velocity (of importance to assess the target stability) has been recently conducted [28], the conditions for non-isobaric ignition being revisited from the Rosen–Lindl gain model.

As shown on the gain curves (figure 12, left), for a given fuel mass, the ignition threshold may be noticeably lowered if the non-isobaric parameter ε (defined by the ratio of the hot spot pressure to the cold shell pressure) is increased. For a DT mass of 0.5 mg (i.e. for roughly the baseline HiPER target), it varies from ∼1 MJ for $\varepsilon = 1$ (with a gain close to 20) to ∼200 kJ for $\varepsilon = 5$ (the gain being then sevenfold). A simple scaling law for the gain G versus the laser energy $E_{\rm las}$ can finally be inferred: $G \propto \varepsilon^{0.27}\alpha^{-0.9}E_{\rm las}^{0.17}(1 - {\rm cst}/E_{\rm las})$. In fact, the ignition conditions were shown to depend both on the spike intensity $I_{\rm s}$ and on the implosion velocity $v_{\rm imp}$, as this quantity is a key parameter for the rebound shock (figure 12, right).

This allows defining a SI operating domain, delimited by the hydrodynamic instabilities at high $v_{\rm imp}$ (but low $I_{\rm s}$) and by the parametric instabilities at high $I_{\rm s}$ (but low $v_{\rm imp}$). Starting with the baseline HiPER target it is thus possible to design a series of homothetic targets, keeping the laser energy, the adiabat and the implosion velocity constant, to explore such a domain and try to minimize the corresponding risks (figure 13) [29].

The two above-mentioned important issues, i.e. the susceptibility of SI to RTI, that may strongly perturb the shell–hot spot interface during the shell deceleration and subsequent stagnation, and to parametric instabilities (the spike intensity

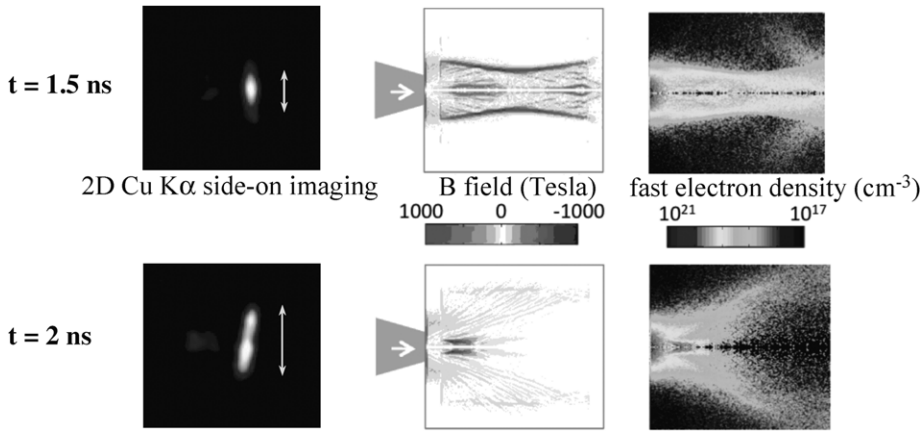

Figure 11. 2D Cu Kα images (left) showing the spread of the electron beam exiting the foam tube (marked by the arrow) increasing when approaching stagnation (bottom—$t = 2$ ns) under the influence of the self-generated magnetic fields (centre).

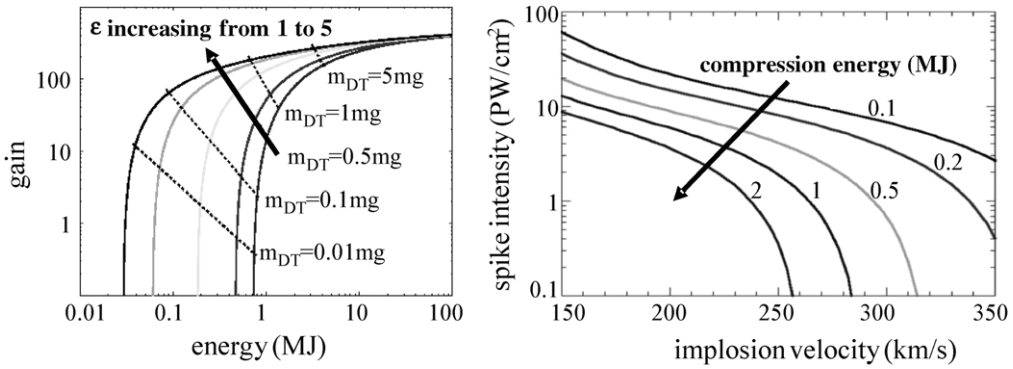

Figure 12. (left) Gain curves for different values of the non-isobaric parameter ε (1, 1.2, 2, 3.5 and 5) assuming an adiabat $\alpha = 2$ and a shell pressure of 200 Gbar. (right) Required spike intensity (PW cm^{-2}) as a function of the implosion velocity (km s^{-1}) for various laser compression.

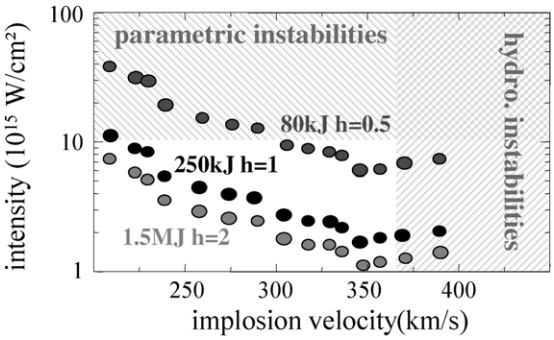

Figure 13. SI operating domain covered by three series of homothetic targets (h-times the reference target in terms of shell radius) requiring laser energies from 80 kJ to 1.5 MJ to ignite.

being above the threshold intensity for SRS and SBS), were addressed through numerical simulations.

The growth of perturbations seeded by a non-isotropic compression has, for instance, been studied. Despite a strong RTI growth observed at ignition time, the HiPER target is igniting [16, 27].

In parallel, 1D large-scale plasma fully kinetic simulations of laser–plasma interaction under SI conditions were performed [30]. The results demonstrate that, after a short initial burst of backscattering, a significant part of the incident laser energy is absorbed in the underdense plasma and transported to denser regions by moderately hot (20–30 keV) electrons. Strong Landau damping suppresses SRS development everywhere in the plasma except in two small regions, near the 1/4th and the 1/16th of the critical density, where an absolute instability can grow locally and whose coupling provides strong feedback and efficient laser energy absorption. Such conditions should not be detrimental to the SI scheme but further studies (to go beyond the mono-dimensional approach and to enlarge the set of laser and plasma parameters) are still required.

The conceptual design of SI has still to be confronted to experiments. Two planar collaborative experiments have already been conducted on European laser facilities but their analyses are still in progress. They both studied shock formation and laser–plasma interaction in well-characterized preformed plasmas (thanks to x-ray laser deflectometry for instance [31]) under laser intensities in the 10^{15}–10^{16} W cm^{-2} range. Shock pressures in the 10 Mbar range were measured at PALS, far below the estimated value notably because of 2D effects and a lack of shock sustainability. In addition, a surprisingly low level of time-integrated backscattering (less than 5%) was recorded [32]. On LULI2000, time-resolved SRS and SBS reflectivities peaking at, respectively, a few per cent and ∼10% were observed (in accordance with previous experiments [10]), while implementation of two VISARs allowed following shock breakouts and coalescence, for code benchmarking (figure 14).

The SI presents then overwhelming advantages: it does not require any complex cone-in-a-shell target nor high-power unconventional lasers, and most of its physics (laser-driven hydrodynamics) is well known and widely experimented. Furthermore, the scheme appears much more robust than initially expected and rather efficient at moderate laser energy, which makes it very attractive for high repetition rate operation.

5. The European DPSSL programme

One of the biggest challenges the HiPER project is facing is to identify a laser architecture that meets all of the demanding requirements. Among those are high wall-plug efficiency (15 to 20%) and repetition rate (5 to 10 Hz) at high energy (∼10 kJ). A diode-pumped solid-state laser (DPSSL) technology programme has thus been initiated in Europe. Different approaches are currently followed [33], differing in gain medium (Yb-doped YAG or calcium fluoride) or amplifier architectures (active mirrors or cooled stack of thin slabs) (figure 15, top), in France (LUCIA at LULI: figure 15, bottom), Germany (POLARIS at IOQ-FSU), the United Kingdom (DIPOLE at STFC) and Czech Republic (HILASE at PALS). Down-selection will occur during the next phase of the HiPER project.

6. Conclusion

Current experiments and target design improvements give confidence in demonstrating indirectly driven ignition at ∼1 MJ on NIF and then LMJ. It will be a major step towards determining the feasibility of ICF as an energy source.

Europe has launched coordinated studies in the framework of the EURATOM keep-in-touch & HiPER programmes to (i) choose the most suitable ignition scheme, thanks to innovative

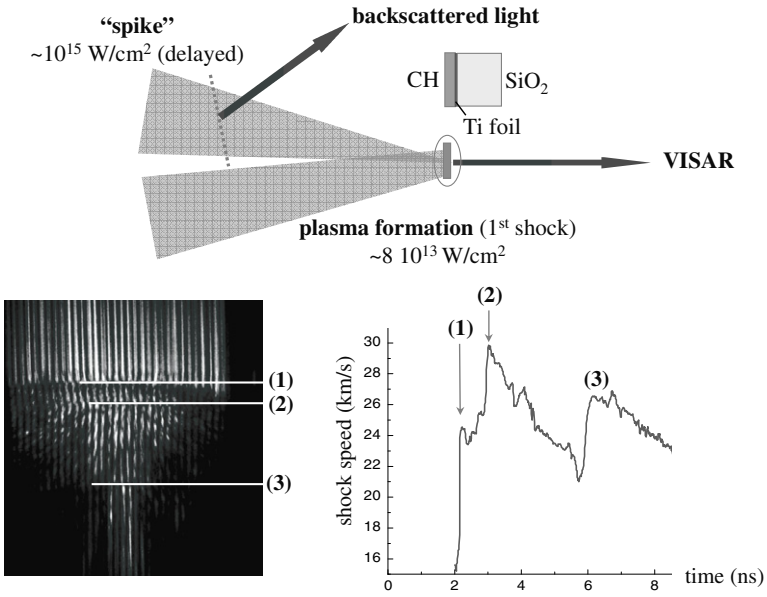

Figure 14. LULI2000 experimental set-up (top) and VISAR image (bottom) showing (1) the 1st moderate shock breakout, (2) its coalescence with the strong shock launched by the spike, as well as (3) a rebound of the 1st shock on, first, the Ti–SiO_2 interface and, then, on the ablation front in the plastic plasma.

DPSSL Programs	Goal Achievement	Gain medium	Amplifier architecture
Germany POLARIS	150 J @ 0.1Hz 12 J @ 0.003 Hz	Yb: CaF_2 crystals	RT° and cryo gas cooled multi-slab
France LUCIA	100 J @ 10Hz 7 J @ 2 Hz	Yb:YAG crystals & ceramics	RT° and cryo gas cooled active mirror
UK DiPOLE	1kJ @ 10 Hz none	Yb:YAG ceramics & glass	cryo gas cooled multi-slab
Czech Republic hilase	100 J @ 10Hz & 6J @ 100Hz none	tbd	tbd

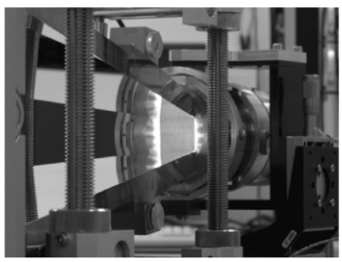

Figure 15. The European DPSSL programme (top); LUCIA Yb : YAG crystal under diode illumination (bottom).

experiments and 2D numerical simulations, (ii) improve diode-pumped solid-state laser driver and target technologies and (iii) design an appropriate IFE reactor. It is currently one of the most interesting places to study ICF thanks to its laser continuum and to these federating activities.

Acknowledgments

The academic studies were partly funded through the EURATOM IFE keep-in-touch programme, the HiPER Preparatory Phase and the LASERLAB-Europe II transnational access programme. The main author (SJ) apologizes for a maybe partial authors' list due to the important number of collaborators involved in this IFE programme.

References

[1] Moses E.I. and Wuest C.R. 2005 *Fusion Sci. Technol.* **47** 314
[2] Ebrardt J. and Chaput J.M. 2010 *J. Phys.: Conf. Ser.* **244** 032017

[3] Collier R. *et al* 2010 *J. Phys.: Conf. Ser.* **244** 032037
[4] Holstein P.A. *et al* 2000 *C. R. Acad. Sci. Paris* IV **1** 693
[5] Nishimura H. *et al* 1993 *Appl. Phys. Lett.* **62** 1344
[6] Vandenboomgaerde M. *et al* 2007 *Phys. Rev. Lett.* **99** 065004
[7] Lafitte S. and Loiseau P. 2010 *Phys. Plasmas* **17** 102704
[8] Cherfils-Clérouin C. *et al* 2010 *J. Phys.: Conf. Ser.* **244** 022009
[9] Seytor P., Galmiche D. and Cherfils C. 2006 *J. Phys.* IV **133** 187
[10] Depierreux S., Michel D.T., Tassin V., Loiseau P., Stenz C. and Labaune C. 2009 *Phys. Rev . Lett.* **103** 115001
[11] Philippe F. *et al* 2010 *Phys. Rev. Lett.* **104** 035004
[12] Dunne M. 2006 *Nature Phys.* **2** 2
[13] Blanchot N. *et al* 2008 *Plasma Phys. Control. Fusion* **50** 124045
[14] Atzeni S. *et al* 2009 *Nucl. Fusion* **49** 055008
[15] Hallo L., Olazabal-Loumé M., Ribeyre X., Dréan V., Schurtz G., Feugeas J.L., Breil J., Nicolaï Ph. and Maire P.H. 2009 *Plasma Phys. Control. Fusion* **51** 014001
[16] Atzeni S., Schiavi A. and Marocchino A. 2011 *Plasma Phys. Control. Fusion* **53** 035010
[17] Temporal M., Canaud B., Laffite S., Le Garrec B.J. and Murakami M. 2010 *Phys. Plasmas* **17** 064504
[18] Depierreux S. *et al* 2009 *Phys. Rev. Lett.* **102** 195005
[19] Atzeni S., Schiavi A., Honrubia J.J., Ribeyre X., Schurtz G., Nicolaï Ph., Olazabal-Loumé M., Bellei C., Evans R.G. and Davies J.R. 2008 *Phys. Plasmas* **15** 056311
[20] Debayle A., Honrubia J.J., d'Humières E. and Tikhonchuk V.T. 2010 *Phys. Rev.* E **82** 036405
[21] Debayle A., Honrubia J.J., d'Humières E., Tikhonchuk V.T., Micheau S. and Geissler M. 2010 *J. Phys.: Conf. Ser.* **244** 022032
[22] Fiuza F., Marti M., Fonseca R.A., Silva L.O., Tonge J., May J. and Mori W.B. 2011 Efficient modelling of laser–plasma interactions in high energy density scenarios *Plasma Phys. Control. Fusion* **53** 074004
[23] Norreys P.A. *et al* 2010 *Plasma Phys. Control. Fusion* **52** 124046
[24] Santos J.J. *et al* 2009 *Plasma Phys. Control. Fusion* **51** 014005
[25] Perez F. *et al* 2009 *Plasma Phys. Control. Fusion* **51** 024035
[26] Volpe L. *et al* 2011 *Plasma Phys. Control. Fusion* **53** 032003
[27] Ribeyre X., Schurtz G., Lafon M., Galera S. and Weber S. 2009 *Plasma Phys. Control. Fusion* **51** 015013
[28] Ribeyre X., Lafon M., Schurtz G., Olazabal-Loumé M., Breil J., Galera S. and Weber S. 2009 *Plasma Phys. Control. Fusion* **51** 124030
[29] Lafon M., Ribeyre X. and Schurtz G. 2010 *Phys. Plasmas* **17** 052704
[30] Klimo O., Weber S., Tikhonchuk V.T. and Limpouch J. 2010 *Plasma Phys. Control. Fusion* **52** 055013
[31] Nejdl J., Kozlová M., Mocek T. and Rus B. 2010 *Phys. Plasmas* **17** 122705
[32] Batani D. *et al* 2011 Laser–plasma coupling in the shock-ignition intensity regime *Acta Technica* at press
[33] Chanteloup J.C. *et al* 2010 *J. Phys.: Conf. Ser.* **244** 012010